Low-temperature dynamics of matrix isolated methane molecules in fullerite C_{60}. The heat capacity, isotope effects

M.I. Bagatskii, V.G. Manzhelii, V.V. Sumarokov, A.V. Dolbin, and M.S. Barabashko

B. Verkin Institute for Low Temperature Physics and Engineering of the National Academy of Sciences of Ukraine
47 Lenin Ave., Kharkov 61103, Ukraine
E-mail: bagatskii@ilt.kharkov.ua

B. Sundqvist

Department of Physics, Umea University, SE - 901 87 Umea, Sweden

The heat capacity of the interstitial solid solution $(CH_4)_{0.4}C_{60}$ has been investigated in the temperature interval 1.4–120 K. The contribution of CH_4 molecules to the heat capacity of the solution has been separated. The contributions of CH_4 and CD_4 molecules to the heat capacity of the solutions $(CH_4)_{0.40}C_{60}$ and $(CD_4)_{0.40}C_{60}$ have been compared. It is found that above 90 K the character of the rotational motion of CH_4 and CD_4 molecules changes from libration to hindered rotation. In the interval 14–35 K the heat capacities of CH_4 and CD_4 molecules are satisfactorily described by contributions of the translational and libration vibrations, as well as the tunnel rotation for the equilibrium distribution of the nuclear spin species. The isotope effect is due to mainly, the difference in the frequencies of local translational and libration vibrations of molecules CH_4 and CD_4. The contribution of the tunnel rotation of the CH_4 and CD_4 molecules to the heat capacity is dominant below 8 K. The isotopic effect is caused by the difference between both the conversion rates and the rotational spectra of the nuclear spin species of CH_4 and CD_4 molecules. The conversion rate of CH_4 molecules is several times lower than that of CD_4 ones. Weak features observed in the curves of temperature dependencies of the heat capacity of CH_4 and CD_4 molecules near 6 and 8 K, respectively, are most likely a manifestation of first-order polyamorphic phase transitions in the orientational glasses of these solutions.

Introduction

Investigations of the physical properties of solid solutions $(CH_4)_nC_{60}$ and $(CD_4)_nC_{60}$ can provide valuable information about the isotopic effects and their role in the low-temperature dynamics of isolated spherical rotators in the octahedral cavities of the low-temperature phase $Pa3$ of the fullerite lattice.

The difference between the molecular masses of methane and deuteromethane is relatively small ($M_{CD4}/M_{CH4} = 1.25$) but the substances differ significantly in moments of inertia ($I_{CD4}/I_{CH4} = 2$), total nuclear spins of the A-, T- and E- species of CH_4 and CD_4 molecules ($S_{CH4} = 2, 1, 0$ and $S_{CD4} = 4, 2, 0$) and magnetic moments of the light atoms ($\mu_H/\mu_D = 3.268$). These differences can cause isotopic effects in the heat capacities $C_{CH4}(T)$ and $C_{CD4}(T)$ of the admixed CH_4 and CD_4 molecules. Substitution of CD_4 for CH_4 in the solutions has a relatively slight effect on the translational subsystem but changes dramatically the physical properties of the rotational subsystem of the CH_4 and CD_4 molecules at helium temperatures at which the quantum effects are dominant.

The low-temperature dynamics of the solutions $(CH_4)_nC_{60}$ and $(CD_4)_nC_{60}$ was investigated by the methods of neutron [1–6] and x-ray [7,8] diffraction, NMR spectroscopy of H [2,3] and ^{13}C [9,10] atoms, dilatometry [11,12] and adiabatic calorimetry [13].

Intercalation of fullerite with CH_4 and CD_4 molecules (and other simple impurities [14–23]) leaves the structures of the high-temperature and low-temperature phases of fullerite unaltered. The lattice parameters of the high-temperature phase of the solutions $(CH_4)_{0.91}C_{60}$ and $(CD_4)_{0.87}$ C_{60} increase at $T \approx 300$ K by 0.026 and 0.016 Å, respectively [2,6], relative to that of pure C_{60} ($a = 14.161$ Å [24]). This depresses the molecular interaction and smears the orientational phase transitions to ~241 K in $(CH_4)_{0.91}C_{60}$ and ~ 235 K in $(CD_4)_{0.87}C_{60}$ [2,6] from ~ 260 K in pure C_{60}. Below these temperatures the third order axes of the C_{60} molecules have the <111> orientations. There are two orientational configurations of C_{60} molecules in which the orientations of the rotation axes of C_{60} differ by 60°. These are symmetrically nonequivalent configurations for C_{60} molecules known as pentagonal (p) and hexagonal (h) [6,25]. The energy difference between the p- and h-configurations is $\Delta E \approx 11$ meV [6,26]. In the orientationally ordered phase the C_{60} molecules execute fast p–h and h–p jumps. As the temperature decreases, the fraction of the p-configurations increases and the frequency of the jumps attenuates. Below the temperature of glass transition ($T_g \approx 90$ K) the p- and h-configurations are frozen and the time of reorientation increases to about an hour [6]. The intercalation of atoms (molecules) to the fullerite C_{60} leads to a change in ΔE and in the p- and h-fractions [6].

Investigations of the thermal expansion $\alpha(T)$ of the solutions $CH_4–C_{60}$ and $CD_4–C_{60}$ show that at $T = 4–6$ K the orientational glasses of these solutions undergo first-order polyamorphic phase transitions evidenced as a hysteresis and maxima in the temperature dependences of $\alpha(T)$ [11,12]. After completing the dilatometric measurements, an x-ray diffraction study of the $CH_4–C_{60}$ sample was performed in the vicinity of the orientational phase transition, $T = 140–320$ K [8].

The dynamics of the solutions $(CH_4)_{0.91}C_{60}$, $(CD_4)_{0.87}C_{60}$ and pure C_{60} was investigated at $T = 1.5–40$ K by Kwei *et al.* [6] using the method of inelastic neutron scattering in the energy range 0.1–100 meV. The energy differences between the lower levels of the rotational spectra of the nuclear spin A-, T- and E-species of CH_4 molecules in the octahedral cavities of C_{60} were measured (see Table 1 in Ref. 6). A nuclear spin conversion of CH_4 molecules was revealed and the time $t_{1/2} \approx 2.6$ h of the conversion between the ground states of the A- and T-species was found. The authors of Ref. 6 analyzed comprehensively their own results and the data [2,9,10] obtained by other methods. It is found that the impurity molecules have a minor effect on the motion of the molecules C_{60}. The CH_4 molecules execute rotational vibrations at helium temperatures and a weakly hindered rotation at $T \sim 120$ K [6].

The heat capacity of the solution $(CD_4)_{0.40}C_{60}$ in the temperature interval 1.2–120 K was measured by Bagatskii *et al.* [13] The results of analysis of the rotational-vibrational states of the CD_4 molecules in the octahedral cavities in fullerite C_{60} [13] are in good agreement with the inelastic neutron scattering [6] and NMR spectroscopic [2,3] data on the dynamics of the molecular motion in the solutions $(CH_4)_{0.92}C_{60}$ and $(CD_4)_{0.88}C_{60}$.

Our goal was to carry out a calorimetric investigation of the isotopic effects in the low-temperature dynamics of admixture molecules in the solid interstitial solutions $(CH_4)_xC_{60}$ and $(CD_4)_xC_{60}$.

Experiment

The heat capacity $C(T)$ of the interstitial solid solution $(CH_4)_{0.40}C_{60}$ was investigated under a constant pressure in the interval $T = 1.5–120$ K. The difference between the heat capacities at constant pressure and volume is negligible for both fullerite and the solution $(CH_4)_{0.40}C_{60}$ below 120 K [24]. The heat capacity $C(T)$ was obtained by subtracting the addenda heat capacity $C_{ad}(T)$ from the total heat capacity $C_{ad+sol}(T)$. The temperature dependence of the $C_{ad}(T)$ (the heat capacity of an "empty" calorimeter with the Apiezon vacuum grease) was measured in a separate experiment [27,28]. The measurements were made by the heat pulse technique using an adiabatic vacuum calorimeter [27]. The variation of the sample temperature was $\Delta T_i = T_{i+1} - T_i$, where T_i and T_{i+1} are the temperatures of the sample before switching on and after switching off heating. It was 0.2–10% of T_i in a single measurement run. The heat capacity corresponds to the average temperature $T = (T_{i+1} + T_i) / 2$. The heating time t_h was 1–10 min. The time required to measure one value of heat capacity was 0.1–0.4 h. This was dictated mainly by the time t_e of equalizing the temperature in the sample after switching off heating. The characteristic time t_m of a single heat capacity measurement was taken to be $t_m = t_h + t_e$. The temperature of the calorimeter was measured with a "CERNOX" thermometer [27,28].

The sample was a cylinder ~8 mm high and 10 mm in diameter. The samples were prepared from a high-purity (99.99%) C_{60} powder (SES, USA) with a grain size of about 0.1 mm. The C_{60} powder was saturated with methane/deuteromethane under similar conditions: $P \approx 200$ MPa and $T = 575$ °C for 36 h. The procedure was performed at the Australian Science and Technology Organization, Australia. The CH_4 or CD_4 molecules filled about 50% of the octahedral cavities in the samples according to thermal gravimetric analysis (TGA). The CH_4 and CD_4–saturated C_{60} powders were compacted at Umea University, Sweden. The technology of sample preparation and estimation

of the methane (deuteromethane) concentration are described in [29,30].

The concentration of admixture CD_4 molecules $n \approx$ $\approx 40\%$ mol was measured in a separate experiment with a low-temperature vacuum desorption gas analyzer [31] after completing the measurement of heat capacity [13]. The design and operation of the gas analyzer is detailed in [31].

The mass of the sample was $m = (874.23 \pm 0,05)$ mg. The sample weighing and mounting in the calorimeter along with hermetization of the vacuum chamber took several hours. Then the vacuum chamber of the calorimeter was washed several times with pure nitrogen gas and the sample was held in the dynamic vacuum at room temperature for ~ 14 h. The residual N_2 pressure in the vacuum chamber was up to several mTorr. The calorimeter was cooled through wires without using He as a heat exchanging gas. The cooling from room temperature to ≈ 5 K took about eight hours. The cooling of the calorimeter from 5 K to about 1.4 K and the reaching a steady–state temperature rate of 10^{-3}–10^{-4} K/min took about 10 h. Several series of measurement were performed. The measurement results were only slightly dependent on the temperature prehistory of the sample.

The measurement error in the heat capacity of $(CH_4)_{0.40}C_{60}$ was $\pm 15\%$ at $T = 1.5$ K, $\pm 4\%$ at $T = 2$ K, and $\pm 2\%$ at $T \geq 4$ K.

Results and discussion

The measured heat capacity $C(T)$ of the solid solution $(CH_4)_{0.40}C_{60}$ normalized to unit mole of C_{60} is shown in Fig. 1 ($T = 1.4$–120 K (a); $T = 1.4$–4 K (b)). The heat capacity C_f of pure fullerite C_{60} added on the figure to comparison has been measured previously in the same calorimeter [27,28]. The heat capacity of the solution increases with temperature in the whole of temperature region. The ratio C/C_f is about 9 at 1.5 K, 5 at 2 K, 2 at 4 K, 1.5 at 20 K, and decreases to 1.3 at 116 K.

Proceeding from the analysis of inelastic neutron scattering data for the $(CH_4)_{0.92}C_{60}$ and $(CD_4)_{0.88}C_{60}$ solutions a conclusion was drawn [6] that intercalation of fullerite with both CH_4 and CD_4 molecules caused only a slight decrease in the frequencies of the translational and libration lattice modes of C_{60}. Therefore, the increase in $C(T)$ against $C_f(T)$ is mainly due to the rotational and translational motion of the CH_4 molecules in the octahedral cavities of the C_{60} lattice.

The dependence $C(T)$ is analyzed assuming that doping of C_{60} with CH_4 molecules has a negligible small effect on the lattice vibrations of the C_{60} molecules [6]. The heat capacity component C_{CH4} was obtained by subtracting $C_f(T)$ of pure C_{60} [13,27] from the heat capacity C of the solution $(CH_4)_{0.40}C_{60}$ ($C_{CH4}(T) = C(T) - C_f(T)$).

The temperature dependence $C_{CH4}(T)$ normalized to the unit mole of CH_4 in the solution is shown in Fig. 2 ($T = 1.4$–120 K (a); $T = 1.4$–18 K (b)) along with the cal-
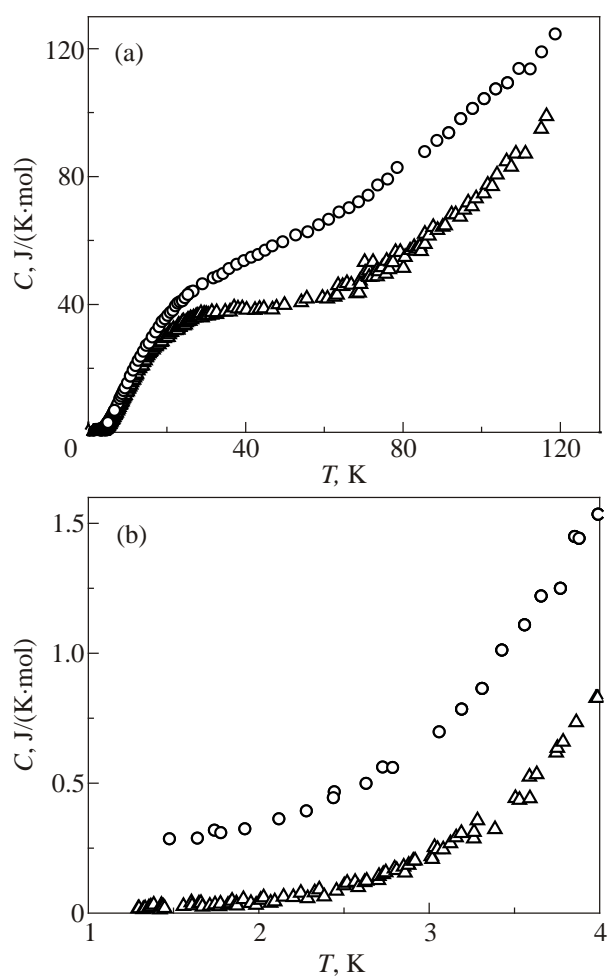
$(CH_4)_{0.40}C_{60}$ (○) and pure fullerite [27] (△) normalized to unit mole of C_{60} in the temperature intervals 1.4–120 K (a) and 1.4–4 K (b).

culated heat capacity curves determined by local translational (C_{tr}, curve *2*) and libration (C_{lib}, curve *3*) vibrations and by tunnel rotation of the CH_4 molecules in the potential field of the octahedral cavities of the C_{60} lattice for the equilibrium ($C_{rot,eq}$, curve *4*) and "frozen" high–temperature ($C_{rot,eq}$, curve *5* in Fig. 2(b)) distributions of the nuclear spin species of the CH_4 molecules. The total heat capacity $C_{calc} = C_{tr} + C_{lib} + C_{rot,eq}$ is described by curve *1*. The C_{tr} and C_{lib} were calculated within the Einstein model. The C_{tr} was calculated using the characteristic Einstein temperature $\Theta_{tr} = 126.5$ K found from inelastic neutron scattering data [6]. The characteristic Einstein temperature $\Theta_{lib} = 67$ K used to calculate C_{lib} was found from the condition of the best fit to $C_{CH4}(T)$. The calculation of $C_{rot,eq}$ and $C_{rot,high}$ is described below. It is seen in Fig. 2(a) that experimental $C_{CH4}(T)$ and calculated C_{calc} agree well in the region $T = 8$–35 K.

As the temperature rises above 35 K, the curve $C_{CH4}(T)$ goes upwards and reaches a maximum at glass-transition temperature ≈ 90 K. On a further increase in the temperature the curve $C_{CH4}(T)$ descends. The fall of $C_{CH4}(T)$ at
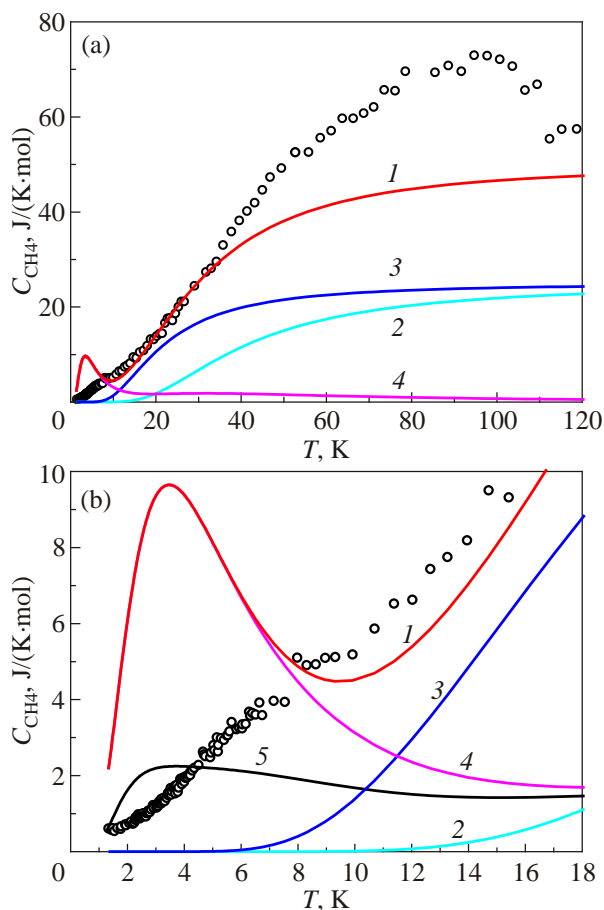
Fig. 2. The contribution $C_{CH4}(T)$ ($\bigcirc$) of the CH$_4$ molecules to the heat capacity $C(T)$ of the solution at $T = 1.4$–120 K (a) and 1.4–18 K (b). The calculated molar heat capacities are determined by local translational (C_{tr}, curve *2*) and libration (C_{lib}, curve *3*) vibrations and tunnel rotation of the CH$_4$ molecules for the equilibrium ($C_{rot,eq}$, curve *4*) and "frozen" high temperature ($C_{rot,high}$, curve *5* in Fig. 2(b)) distributions of the nuclear spin species. The total heat capacity $C_{calc} = C_{tr} + C_{lib} + C_{rot,eq}$ is described by curve *1*.

$T > 90$ K occurs because the rotational motion of the CH$_4$ molecules changes from libration to hindered rotation.

At $T = 35$–120 K the calculated heat capacity C_{calc} is lower than $C_{CH4}(T)$. As for the solution (CD$_4$)$_{0.40}$(C$_{60}$), we assume that the discrepancy may be due to "additional" rotational excitations of the CH$_4$ molecules in the region of a phase transition from a glass state to an orientationally ordered phase. According to Ref. 6, the motion of CH$_4$ molecules has a weak effect on the translational and rotational lattice vibrations of the C$_{60}$ molecules in the solution; on the contrary, the motion of the C$_{60}$ molecules affects appreciably the local translational and rotational vibrations of the CH$_4$ molecules. The formations of an orientation glass in the solution (CH$_4$)$_{0.40}$C$_{60}$ changes the character of the rotational motion of the C$_{60}$ molecules, which induces the "additional" rotational excitations of the CH$_4$ molecules.

The contribution of the tunnel rotation of the CH$_4$ molecules to $C_{CH4}(T)$ dominates below 8 K (see Fig. 2(b)).

At $T < 8$ K the heat capacity $C_{CH4}(T)$ is determined by the low-lying energy levels of the rotational spectra of the nuclear spin *A*-, *T*- and *E*-species of the CH$_4$ molecules and by the correlation between the characteristic time τ_{CH4} of CH$_4$ conversion and the time t_m of one measurement run [32,33]. The low-energy parts of the rotational spectra of the *A*-, *T*- and *E*-species of CH$_4$ are as for CD$_4$ dependent on the symmetry and value of the crystal field. The rotators CH$_4$ and CD$_4$ are therefore an effective probe of the crystal environment in the octahedral cavities of the fullerite C$_{60}$. The *A*-species has the lowest–energy state. Therefore, under the equilibrium condition at $T = 0$ K all the CH$_4$ molecules are in this state. At $T > 0$ K the equilibrium distribution of the *A*-, *T*- and *E*- species is reached through state conversion.

The energy differences between the low-lying energy levels of the *A*-, *T*- and *E*- species of the CH$_4$ molecule in the octahedral cavity of the lattice in the solution (CH$_4$)$_{0.92}$(C$_{60}$) were found by the method of inelastic neutron scattering [6] (see Table 1 in Ref. 6). It is found [6] that (i) the rotational spectra are close in the *p*- and *h*-configurations; (ii) the relaxation time of the occupancy of rotational energy levels above the ground state of the *A*- and *T*-species of CH$_4$ molecules is rather short; (iii) the time of conversion between the ground states of the *A*- and *T*-species of CH$_4$ molecules at $T \approx 4$ K is $t_{1/2} \approx 2.6$ h. A two-parameter model of a crystal potential field $V(w) = = B_{CH4}[\beta_4 V_4(w) + \beta_6 V_6(w)]$ in the octahedral cavity of C$_{60}$ was proposed. Here the $B_{CH4} = 7.538$ K is the rotational constant of the CH$_4$ molecule, $V_4(w)$, $V_6(w)$ are basis functions with symmetry $\bar{A}_1 A_1$ and β_4, β_6 are the dimensionless parameters. Proceeding from the available experimental data and assuming $\beta_4 = 2.1856\beta_6$ Kwei et. al. calculated the energies of some low-lying levels in the rotational spectra of the *A*-, *T*- and *E*-species of CH$_4$ molecules as a function of the potential field parameters (β_4, β_6) (see Fig. 1 in Ref. 6).

Figure 3 illustrates our estimates (based on the data of Table 1 in [6]) of the low-energy parts of the rotational spectra of CH$_4$ molecules in the octahedral cavity of fullerite C$_{60}$. The $C_{rot,eq}(T)$ (Fig. 2(a), curve *4*) was calculated for the case of "fast" conversion ($\tau_{CH4} << t_m$) when the concentration distribution of the nuclear spin species of CH$_4$ at the test temperature can be considered as being in equilibrium at any moments. This occurs when the conversion is completed within the effective time t_m of a single measurement. Under such a condition the heat capacity can

Table 1. The Einstein temperatures of translational ($\Theta_{CH4,tr}$, $\Theta_{CD4,tr}$) and librational ($\Theta_{CH4,lib}$, $\Theta_{CD4,lib}$) vibrations of CH$_4$ and CD$_4$ [13] molecules in octahedral cavities of fullerite C$_{60}$.

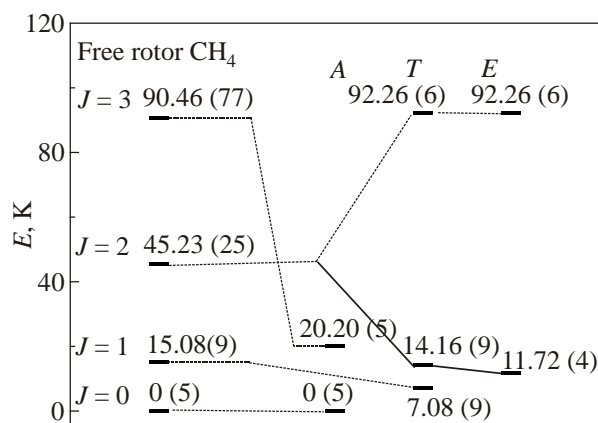| Sample	Θ_{tr}, K	Θ_{lib}, K
CH$_4$	126.5	67
CD$_4$	112.6	51

Fig. 3. The low-energy part of the rotational spectrum of free CH_4 molecules [34] and for CH_4 molecules in the potential field of the octahedral cavities in C_{60} [6] for the A-, T- and E- nuclear spin species. J is the rotational quantum number and E is the energy (the degeneracy of the energy levels are shown in parentheses to the right).

be calculated using a unified rotational energy spectrum including all species levels.

The $C_{rot,high}(T)$ was calculated (see Fig. 2(b), curve *5*) for the case when there is no conversion ($\tau_{CH4} \gg t_{ex} \gg t_m$). Under this condition the distribution of species remains constant during the measurement time t_m (several weeks) in the whole temperature region and is equal to the high-temperature "frozen" distribution $x_A:x_B:x_E = 5:9:2$. Therefore, $C_{rot,high}(T) = (5/16)C_A(T) + (9/16)C_T(T) + (2/16)C_E(T)$, where the molar heat capacities $C_{A,rot}(T)$, $C_{T,rot}(T)$, $C_{E,rot}(T)$ depend only on the transitions inside each species.

It is seen in Fig. 2(b) that the experimental heat capacity $C_{CH4}(T)$ is inconsistent with the calculated curves $C_{rot,eq}(T)$ and $C_{rot,high}(T)$. At $\tau_{CH4} \sim t_m$ the heat capacity $C_{CH4}(T)$ depends on the number of CH_4 molecules which convert during the time t_m [32]. The characteristic time $\tau_{CH4}(T)$ of the conversion in CH_4 molecules can be described as

$$\tau_{CH4}(T) = -t_m / \ln(1 - K') , \qquad (1)$$

where $K' = C_{CH4}(T) / C_{rot,eq}(T)$ is the fraction of CH_4 molecules in the equilibrium distribution that converted during the time t_m.

The time of cooling of the calorimeter from 5 to 1.4 K and achieving a steady-state rate of temperature was about 10 h. During this period the CH_4 species came to a near-equilibrium distribution over the sample. Most of the CH_4 molecules were in the ground state of the A-species. In our experiment $\tau_{CH4} \approx t_m$ and $C_{CH4}(T)$ is determined by the number of CH_4 molecules which converted during the effective time t_m of a single heat capacity measurement [32].

Above 8 K $C_{CH4}(T)$ corresponds to the equilibrium distribution of CH_4 species. The relatively fast drop of the theoretical $C_{rot,eq}(T)$ values in the region $T = 8$–12 K suggests that the higher-lying energy levels of the molecules

CH_4 (than for those shown in Fig. 3) are ignored in calculation of $C_{rot,eq}(T)$.

We estimated $K' = C_{CH4}(T) / C_{rot,eq}(T)$ and the average experimental times t_m at $T = 2$–7.5 K. The temperature dependence of the characteristic conversion time $\tau_{CH4}(T)$ of the CH_4 molecules in the octahedral cavities of C_{60} was calculated using the $K'(T)$ and $t_m(T)$ values according Eq. (1). The dependences $\tau_{CH4}(T)$ and $\tau_{CD4}(T)$ [13] for the solutions $(CH_4)_{0.40}C_{60}$ and $(CD_4)_{0.40}C_{60}$ are illustrated in Fig. 4. The curves are in good qualitative agreement. The $\tau_{CH4}(T)$ and $\tau_{CD4}(T)$ decrease with rising temperature. At $T = 4$ K $\tau_{CH4}(T)$ is about 5.5 times lower than $t_{1/2}$ and about 4.7 times higher than $\tau_{CD4}(T)$ [13].

The isotopic effects in $C_{CH4}(T)$ and $C_{CD4}(T)$ are illustrated in Fig. 5 ($T = 1.2$–120 K (a); $T = 1.2$–18 K (b)). In the interval $T = 12$–40 K the isotopic effect is mainly due to the frequency difference between the local translational and libration vibrations of CH_4 and CD_4 molecules. The Einstein temperatures of the translational ($\Theta_{CH4,tr}$, $\Theta_{CD4,tr}$) and libration ($\Theta_{CH4,lib}$, $\Theta_{CD4,lib}$) vibrations of CH_4 and CD_4 molecules are given in Table 1.

In the region of formation of the orientational phase transition from a glass state to an orientationally ordered phase of fullerite C_{60} ($\Delta T = 40$–100 K) $C_{CD4}(T)$ and $C_{CH4}(T)$ are influenced by "additional" excitations of CH_4 and CD_4 molecules (Fig. 5(a)). These excitations appear because the motion of the C_{60} molecules in the lattice fullerite and the motion of the impurity molecules are coupled.

At $T = 80$–120 K the curve $C_{CH4}(T)$ is higher than the curve $C_{CD4}(T)$ (Fig. 5(a)). This may be due to an uncertainty in the CH_4 concentrations. The behavior of $C_{CD4}(T)$ and $C_{CH4}(T)$ correlates with the effects of the impurity molecules CH_4 and CD_4 on change of the lattice parameter of C_{60}. At $T \sim 300$ K the lattice parameter of the solutions $(CH_4)_{0.91}C_{60}$ and $(CD_4)_{0.87}C_{60}$ increases by 0,026 Å and 0,016 Å [6], respectively, relative to that of pure C_{60} ($a = 14{,}161$ Å) [24].
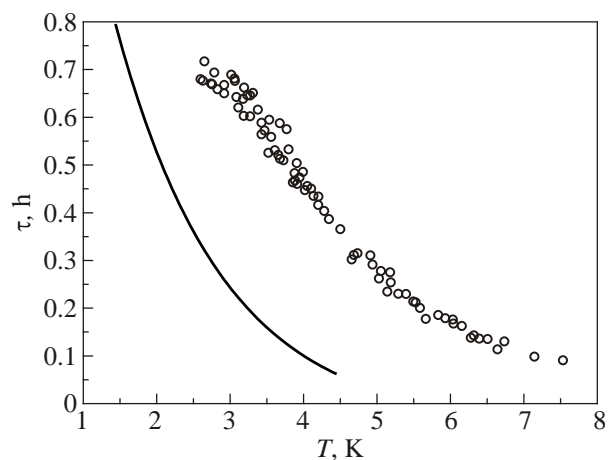

Fig. 4. The characteristic conversion times $\tau_{CH4}(T)$ ($\bigcirc$) and $\tau_{CD4}(T)$ [13] (solid line) of CH_4 and CD_4 molecules in the octahedral cavities of fullerite.
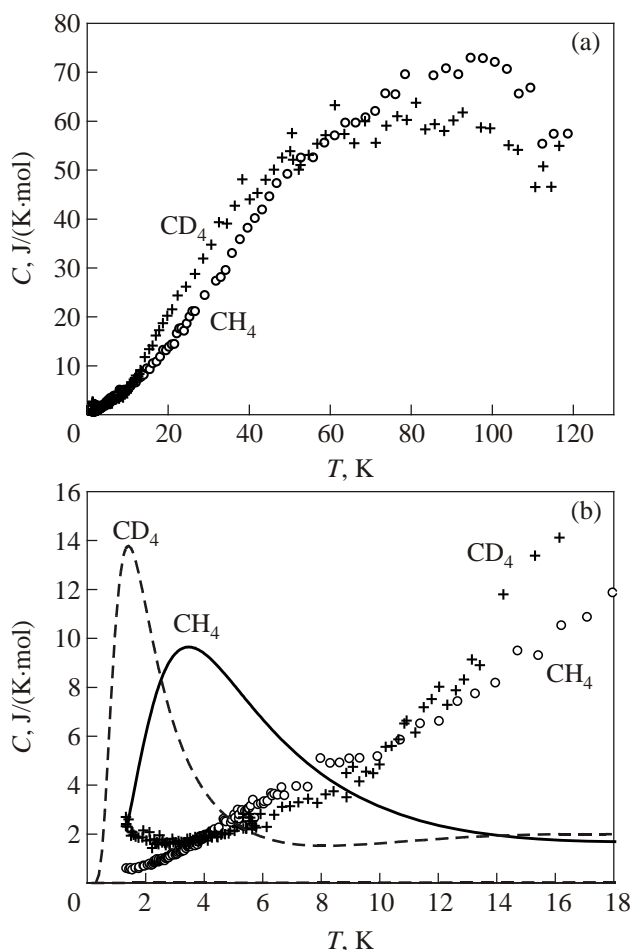
Fig. 5. The isotopic effects in $C_{CH4}(T)$ ($\bigcirc$) and $C_{CD4}(T)$ [13] (+) at $T = 1.2{-}120$ K (a) and $T = 1.2{-}18$ K (b). The solid and dashed curves in Fig. 5(b) are the calculated heat capacities $C_{rot,eq}$ determined by tunnel rotation of CH_4 and CD_4 molecules, respectively, in the case of the equilibrium distribution of the nuclear spin species.*Fig. 1.* The heat capacities of the solid solution

The $C_{CH4}(T)$ and $C_{CD4}(T)$ exhibit a complex isotopic effect below 14 K (Fig. 5(b)) when the contributions of the translational and libration modes decrease exponentially and quantum regularities scale up to a macroscopic level. The dependences $C_{CH4}(T)$ below 8 K and $C_{CD4}(T)$ below 6 K are determined by the tunnel rotation of the CH_4 and CD_4 molecules. The isotope effect is due to differences between both the rates of conversion (see Fig. 4) and rotational spectra of nuclear spin modifications of molecules CH_4 and CD_4 (see Fig. 3 in this article and Fig. 4 in Ref. 13). The rotational constant of CH_4 molecules is twice as large as that of CD_4 molecules. Therefore, the distance between the rotational tunnel energy levels of the CH_4 species is also twice that in the case of CD_4. The differences in the level degeneracy are due to the different total nuclear spin species of the molecules. In the case of an equilibrium distribution of CH_4 and CD_4 species the isotopic effect in $C_{CH4}(T)$ and $C_{CD4}(T)$ makes itself evident in the differences between the curves describing $C_{rot,eq}$

(Fig. 5(b), solid curve for CH_4 and dashed curve for CD_4). Besides, below 5 K the conversion rate of CD_4 molecules is several times higher than that of CH_4 molecules (Fig. 4). The conversion of molecules deuteromethane has been first found in the solid solutions $(CD_4)_x$Kr [35,36]. The behavior of the experimental temperature dependences $\tau_{CH4}(T)$ and $\tau_{CD4}(T)$ [13], as in cases of solid solutions $(CH_4)_x$Kr [32,33], $(CD_4)_x$Kr [35,36], agrees qualitatively with the theoretical data on conversion in multiatomic molecules.

In contrast to diatomic molecules [37–40], other mechanisms of conversion are dominant in multiatomic molecules at low temperatures. These are hybrid [41] and "quantum relaxation" [42,43] mechanisms. According to the theory of the hybrid conversion mechanism [41], the highest conversion rate is determined by the intramolecular magnetic interaction of protons and the intermolecular noncentral interaction between the nearest molecules in the lattice. The intramolecular interaction mixes the nuclear spin states, while the intermolecular noncentral interaction induces transitions between the rotational states transferring the conversion energy to the lattice. The hybrid mechanism is dominant at low temperatures [41]. The noncentral interaction between CD_4 and C_{60} molecules is more than in case of CH_4 and C_{60} molecules. This is because CD_4 molecules have smaller amplitudes of zero-point orientational vibrations and a larger effective electric octupole moment in the ground state. Therefore, the probability of conversion energy transfer from the CD_4 molecules to the C_{60} lattice is higher than in the case of CH_4 molecules. Hence, CD_4 molecules have a higher conversion rate.

The contribution of the "quantum relaxation" mechanism of conversion increases with temperature [42,43]. The conversion rate is determined by the intramolecular magnetic interaction of proton (deuteron) and the tunnel exchange of the states of the species having equal energy levels (no phonons are involved). The distance between the lowest-lying rotational levels of the CD_4 molecules is half as large as that in case of CH_4 molecules (see Fig. 3 in this work and Fig. 4 in Ref. 13). Therefore, at equal temperatures below 5 K the conversion rate of CD_4 is higher than that of CH_4. In the regions $T = 1.3{-}5.5$ K and $T = 1.4{-}8$ K the experimental heat capacities $C_{CD4}(T)$ and $C_{CH4}(T)$ are dependent on the number of the molecules which converted during the effective time t_m of a single run of heat capacity measurement [32]. The heat capacities $C_{CD4}(T)$ above ≈ 5.5 K and $C_{CH4}(T)$ above ≈ 8 K correspond to the equilibrium distribution of the molecular species.

It is interesting that at $T = 5{-}6$ K and $T = 7{-}8$ K the scatter of the $C_{CD4}(T)$ and $C_{CH4}(T)$ data, respectively, is considerably wider than at the other temperatures. This may be due to the first-order phase transitions in the orientational glasses of the CH_4–C_{60} and CD_4–C_{60} solutions [11,12].

Conclusions

The heat capacity of CH_4 intercalated fullerite $(CH_4)_{0.4}C_{60}$ has been first investigated in the interval 1.4–120 K. The contribution $C_{CH4}(T)$ of the CH_4 molecules isolated in the octahedral cavities of the C_{60} lattice to the heat capacity of the solution has been separated. The contributions of the CH_4 and CD_4 to the heat capacity of the solutions $(CH_4)_{0.4}C_{60}$ and $(CD_4)_{0.4}C_{60}$ have been compared.

It has been found that above 90 K the rotational motion of the CH_4 and CD_4 molecules changes from librational vibrations to a hindered rotation. The heat capacities $C_{CH4}(T)$ in the range from 8 to 35 K and $C_{CD4}(T)$ in $T = 14$–35 K are described well taking into account the contributions of translational and librational vibrations, as well as the tunnel rotation of the CH_4 and CD_4 molecules in the case of an equilibrium distribution of the nuclear spin species. The isotopic effect is caused mainly by the frequency differences between the local translational and libration vibrations of the CH_4 and CD_4 molecules.

The characteristic conversion times of the lowest-lying levels of the CH_4 species have been estimated at $T < 7$ K. The isotopic effect in $C_{CH4}(T)$ and $C_{CD4}(T)$ is induced by the differences between both the conversion rates and the rotational spectra of the nuclear spin species of the CH_4 and CD_4 molecules.

The weak features observed in the curves $C_{CH4}(T)$ near 6 K and $C_{CD4}(T)$ near 8 K are most likely manifestations of first-order phase transition in the orientational glasses of the solutions [11,12].

1. J.E. Schirber, G.H. Kwei, J.D. Jorgensen, R.L. Hitterman, and B. Morosin, *Phys. Rev. B* **51**, 12014 (1995).

2. B. Morosin, J.D. Jorgensen, S. Short, G.H. Kwei, and J.E. Schirber, *Phys. Rev. B* **53**, 1675 (1996).

3. B. Morosin, R.A. Assink, R.G. Dunn, T.M. Massis, J.E. Schirber, and G.H. Kwei, *Phys. Rev. B* **56**, 13611 (1997).

4. W.I.F. David, R.M. Ibberson, T.J.S. Dennis, J.P. Hare, and K. Prassides, *Europhys. Lett.* **18**, 219 (1992).

5. W.I.F. David, R.M. Ibberson, and T. Matsuo, *Proc. R. Soc. London, Ser. A* **442**, 129 (1993).

6. G.H. Kwei, F. Troun, B. Morosin, and H.F. King, *J. Chem. Phys.* **113**, 320 (2000).

7. P.A. Heiney, J.E. Fischer, A.R. McGhie, W.J. Romanow, A.M. Denenstein, J.P. McCauley, Jr., A.B. Smith, and D.E. Cox, *Phys. Rev. Lett.* **66**, 2911 (1991).

8. N.A. Aksenova, N.N. Galtsov, and A.I. Prokhvatilov, *Fiz. Nizk. Temp.* **38**, 278 (2012) [*Low Temp. Phys.* **38**, 221 (2012)].

9. R. Tycko, G. Dabbagh, R.M. Fleming, R.C. Haddon, A.V. Makhija, and S.M. Zahurak, *Phys. Rev. Lett.* **67**, 1886 (1991).

10. R.D. Johnson, C.S. Yannoni, H.C. Dorn, J.R. Salem, and D.S. Bethune, *Science* **255**, 1235 (1992).

11. A.V. Dolbin, V.B. Esel`son, V.G. Gavrilko, V.G. Manzhelii, N.A. Vinnikov, G.E. Gadd, S. Moricca, D. Cassidy, and B. Sundqvist, *Fiz. Nizk. Temp.* **33**, 1401 (2007) [*Low Temp. Phys.* **33**, 1068 (2007)].

12. A.V. Dolbin, N.A. Vinnikov, V.G. Gavrilko, V.B. Esel'son, V.G. Manzhelii, G.E. Gadd, S. Moricca, D. Cassidy, and B. Sundqvist, *Fiz. Nizk. Temp.* **35**, 299 (2009) [*Low Temp. Phys.* **35**, 226 (2009)].

13. M.I. Bagatskii, V.V. Sumarokov, A.V. Dolbin, and B. Sundqvist, *Fiz. Nizk. Temp.* **38**, 87 (2012) [*Low Temp. Phys.* **38**, 67 (2012)].

14. T.B. Tang and M. Gu, *Fiz. Tverd. Tela* **44**, 607 (2002).

15. Yu.E. Stetsenko, I.V. Legchenkova, K.A. Yagotintsev, A.I. Prokhvatilov, and M.A. Strzhemechny, *Fiz. Nizk. Temp.* **29**, 597 (2003) [*Low Temp. Phys.* **29**, 445 (2006)].

16. G.E. Gadd, S.J. Kennedy, S. Moricca, C.J. Howard, M.M. Elcombe, P.J. Evans, and M. James, *Phys. Rev. B* **55**, 14794 (1997).

17. G.E. Gadd, S. Moricca, S.J. Kennedy, M.M. Elcombe, J. Evans, M. Blackford, D. Cassidy, C.J. Howard, P. Prasad, J.V. Hanna, A. Burchwood, and D. Levy, *J. Phys. Chem. Solids* **58**, 1823 (1997).

18. M. Gu and T.B. Tang, *J. Appl. Phys.* **93**, 2486 (2003).

19. K.A. Yagotintsev, Yu.E. Stetsenko, I.V. Legchenkova, A.I. Prokhvatilov, M.A. Strzhemechny, E. Schafler and M. Zehetbauer, *Fiz. Nizk. Temp.* **35**, 315 (2009) [*Low Temp. Phys.* **35**, 239 (2009)].

20. B. Renker, H. Schober, M.T. Fernandez-Diaz, and R. Heid, *Phys. Rev. B* **61**, 13960 (2000).

21. N.N. Galtsov, A.I. Prokhvatilov, G.N. Dolgova, D. Cassidy, G.E. Gadd, and S. Moricca, *Fiz. Nizk. Temp.* **33**, 1159 (2007) [*Low Temp. Phys.* **33**, 881 (2007)].

22. I. Holleman, G. von Helden, E.H.T. Olthof, P.J.M. van Bentum, R. Engeln, G.H. Nachtegaal, A.P.M. Kemtgens, B.H. Meier, A. van der Avoird, and G. Meijer, *Phys. Rev. Lett.* **79**, 1138 (1997).

23. I. Holleman, *Dynamics of CO in solid C$_{60}$, Thesis Katholieke Universiteit Nijmegen*, (1998) (in Dutch).

24. N.A. Aksenova, A.P. Isakina, A.I. Prokhvatilov, and M.A. Strzhemechny, *Fiz. Nizk. Temp.* **25**, 964 (1999) [*Low Temp. Phys.* **25**, 784 (1999)].

25. W.I.F. David, R.M. Ibberson, T.J.S. Dennis, J.P. Hare, and K. Prassides, *Europhys. Lett.* **18**, 219 (1992).

26. S. van Smaalen, R. Dinnebier, I. Holleman, G. von Helden, and G. Meijer, *Phys. Rev. B* **57**, 6321 (1998).

27. M.I. Bagatskii, V.V. Sumarokov, and A.V. Dolbin, *Fiz. Nizk. Temp.* **37**, 535 (2011) [*Low Temp. Phys.* **37**, 424 (2011)].

28. M.I. Bagatskii, V.V. Sumarokov, and A.V. Dolbin, in: *Abstracts 8th Conference of Cryocrystals and Quantum Crystals CC-2010*, Chernogolovka, Russia (2010), P. 61.

29. G.E. Gadd, S. Moricca, S.J. Kennedy, M.M. Elcombe, P.J. Evans, M. Blackford, D. Cassidy, C.J. Howard, P. Prasad, J.V. Hanna, A. Burchwood, and D. Levy, *J. Phys. Chem. Solids* **58**, 1823 (1997).

30. A.N. Aleksandrovskii, A.S. Bakai, D. Cassidy, A.V. Dolbin, V.B. Esel'son, G.E. Gadd, V.G. Gavrilko, V.G. Manzhelii,

S. Moricca, and B. Sundqvist, *Fiz. Nizk. Temp.* **31**, 565 (2005) [*Low Temp. Phys.* **31**, 429 (2005)].

31. A.M. Aleksandrovskii, M.A. Vinnikov, V.G. Gavrilko, O.V. Dolbin, V.B. Esel'son, and V.P. Maletskiy, *Ukr. J. Phys.* **51**, 1152 (2006).

32. M.I. Bagatskii, V.G. Manzhelii, I.Ya. Minchina, D.A. Mashchenko, and I.A. Gospodarev, *J. Low Temp. Phys.* **130**, 459 (2003).

33. I.Ya. Minchina, M.I. Bagatskii, V.G. Manzhelii, O.V. Sklyar, D.A. Mashchenko, and M.A. Pokhodenko, *Fiz. Nizk. Temp.* **27**, 773 (2001) [*Low Temp. Phys.* **27**, 568 (2001)].

34. E.B. Wilson, *J. Chem. Phys.* **3**, 276 (1935).

35. M.I. Bagatskii, V.G. Manzhelii, D.A. Mashchenko, V.V. Dudkin, *Fiz. Nizk. Temp.* **29**, 216 (2003) [*Low Temp. Phys.* **29**, 159 (2003)].

36. M.I. Bagatskii, V.G. Manzhelii, V.V. Dudkin, D.A. Mashchenko, and S.B. Feodosyev, *Fiz. Nizk. Temp.* **29**, 1352 (2003) [*Low Temp. Phys.* **29**, 1028 (2003)].

37. K. Motizuki, *J. Phys. Soc. Jpn* **12**, 163 (1957).

38. K. Motizuki and T. Nagamiya, *J. Phys. Soc. Jpn*. **11**, 93 (1956).

39. M.I. Bagatskii, A.I. Krivchikov, V.G. Manzhelii, I.Ya. Minchina, and P.I. Muromtsev, *Fiz. Nizk. Temp.* **13**, 1001 (1987) [*Sov. J. Low Temp. Phys.* **13**, 571 (1987)].

40. M.A. Strzhemechny and O.I. Tokar, *Fiz. Nizk. Temp.* **11**, 813 (1985) [*Sov. J. Low Temp. Phys*. **11**, 446 (1985)].

41. A.J. Nijman and A.J. Berlinsky, *Canad. J. Phys.* **58**, 1049 (1980).

42. R.F. Curl, J.V.V. Kasper, and K.S. Pitzer, *J. Chem. Phys.* **46**, 3220 (1967).

43. P.L. Chapovssky and L.J.F. Hermans, *Annu. Rev. Phys. Chem.* **50**, 315 (1999)